

Optimizing Ocean Energy Harvesting: The Significance of Natural Frequency in Piezoelectric Generator Device Electrical Output

Ede Mehta Wardhana¹, Meitha Soetardjo², Semin³, Agoes Santoso⁴, Sutopo P Fitri⁵
(Received: 07 November 2023 / Revised: 12 November 2023 / Accepted: 23 November 2023)

Abstract— This study explores the significance of the natural frequency parameter in enhancing the electrical performance of a piezoelectric generator device, mainly when deployed in ocean energy harvesting. While natural energy harvesting aims to establish affordable and sustainable renewable energy sources, piezoelectric devices capitalize on the inherent piezoelectric effect derived from natural movements. Despite the abundance of constant natural movements in the Earth's environment, the application of piezoelectric devices in ocean energy remains relatively understudied. The experimental setup involves a cantilever-designed piezoelectric device made from polyvinylidene fluoride (PVDF). The study investigates the relationships between vibration frequency, initial distance, and electrical output. Findings indicate that higher setup parameters may lead to increased electrical output, but the relationship is not linear. Notably, the resonance between the vibration frequency and the device's natural frequency emerges as a critical factor in optimizing electrical performance. Detailed experimentation, visualized through figures and graphs, demonstrates the nuanced interplay of setup parameters and electrical output. The study emphasizes that the initial distance, while important, does not singularly determine the device's electrical performance. It challenges conventional beliefs by showcasing that piezoelectric devices can operate efficiently in tight spaces. Furthermore, the study delves into the non-linear relationship between vibration frequency and electrical output. Examining natural and resonant frequencies reveals that resonance occurs most prominently at the device's natural frequency, emphasizing the importance of precise tuning for optimal performance. The findings offer valuable insights for the strategic deployment of piezoelectric technology in ocean energy harvesting, paving the way for more efficient and effective devices in real-world conditions.

Keywords— Piezoelectric generator, piezoelectric, natural frequency, vibration frequency, ocean energy harvesting

I. INTRODUCTION

Natural energy harvesters primarily focus on developing a new, affordable, sustainable, readily maintained renewable energy source. These goals have been steadily progressing and produced various devices that mainly focus on alternative energy. Piezoelectric devices are developed based on the piezoelectric effect from the natural movement of things or absorbed from the natural movement of nature. The device could generate electricity when the pressure is applied. Since the earth has plenty of constant natural movement (for example, the wind blowing, constant movement of the ocean waves, or waterfall motions), there is no shortage of sources for Piezoelectric devices.

Similarly, ocean energy applications also rapidly advanced. Since the ocean possesses various movements, magnitudes, and frequencies, various methods could be implemented to absorb and convert the motions into useful energy (such as mechanical or electrical energy). Despite the similarity, the utilization of piezoelectric

devices in the blue energy field is still considered a minimum or limited studies.

Numerous research, development, and prototyping have been developed and applied, such as the use of piezoelectric plate in traversing the ocean, piezoelectric coupled buoy structure model, and piezoelectric coupled to a coastal structure [1]–[3] for an energy collecting process in the deep and intermediate oceans from wave motions. An investigation conducted in [4], [5] for the piezoelectric device generator with a cantilever-supported beam as its core model was also implemented to see the results of the electrical power generated from the ocean. Additionally, the potential ability for piezoelectric device electrical power generation is also investigated in [6] which then originated several unique models such as a small subsurface ocean/river power generator, “eel” shaped bluff body installed under ocean waves and fork-shaped bluff body model [7]–[9]. Several reviews that describe the advantages and disadvantages and various improvements of the previous piezoelectric devices also can be read in [10]–[14].

Ede Mehta Wardhana, Departement of Marine Engineering, Institut Teknologi Sepuluh Nopember, Surabaya 601111, Indonesia.
E-mail:ede@ne.its.ac.id

Meitha Soetardjo, National Research and Innovation Agency (BRIN), Surabaya 601111, Indonesia.
E-mail: meithasoetardjo@gmail.com

Semin, Departement of Marine Engineering, Institut Teknologi Sepuluh Nopember, Surabaya 601111, Indonesia.
E-mail: seminit@yahoo.com

Agoes Santoso, Departement of Marine Engineering, Institut Teknologi Sepuluh Nopember, Surabaya 601111, Indonesia.
E-mail: agoes@its.ac.id

Sutopo Purwono Fitri, Departement of Marine Engineering, Institut Teknologi Sepuluh Nopember, Surabaya 601111, Indonesia.
E-mail: sutopopf@gmail.com

Even though there are various studies investigating the most suitable model, the motion and movement of the ocean for the energy absorption, and the electrical power generated by the piezoelectric device on the ocean field, there is still a lack of understanding in what factors that could influence the power generation itself. There is still not enough comprehension of what causes the improvement of power generation, the consideration when deploying the device in the ocean field, and, more importantly, the variables that need to be understood in order to create a much more efficient and effective piezoelectric device for harvesting the ocean energy.

In this study, we examined the electrical energy generation from our proposed piezoelectric device. We measured the electricity results based on the external vibration motion from the machine as an illustration of how the natural movement from the ocean could translate into electricity from the device. The focus of this study is to investigate the characteristics of electrical energy generation and, more significantly, what variables or factors could influence the results. This study is the continuation of our previous works in [15]. Several figures and graphs are extracted from that work with additional information regarding the importance, and the foremost point in this paper is added. The relations between the setup parameters and the magnitude of electrical voltage were shown to inform the relations between that specific parameter and the piezoelectric device's voltage.

II. METHOD

This study was conducted and examined by conducting experiments. Therefore, in order to elucidate the process of the experiments, there are three parts of the setup :

A. Piezoelectric device setup

Firstly, we explain the setup or how we developed the piezoelectric device used in this study. An individual piezoelectric device made from the polyvinylidene fluoride (PVDF) layer with a thickness of 40 to 100 μm was used as the core for our piezoelectric device. To protect the PVDF layer and ensure its flexibility, a double-thin elastic silicone rectangle was put on the bottom and top of the PVDF. A cable was also attached to the right end of the PVDF layer to carry the electricity production and to measure that same electrical energy from the piezoelectric device motions. Figure 1. displays the completed piezoelectric device in this experiment. The PVDF layer dimensions are 15 cm x 5 cm, while both silicone layer dimensions are 20 cm x 6 cm.

Additionally, since the piezoelectric device created in this study is based on the cantilever-design model, four 2-mm diameter holes are also created. Two holes are located on the left side of the elastic silicone layer, while the remaining holes are located on the right side. This hole will help to limit the movement of the piezoelectric device depending on which setup from our experiments; by limiting one side of the device, we hypothesize the bending motion can be higher, and in turn, the pressure and electrical power generation could be higher as well.

B. External mechanical motions and measurement setup

We conducted vibration tests using a vibration generator to examine the fundamental characteristics of the piezoelectric device. The vibration generator will generate movement according to the stroke and frequencies as variables. Those variables will illustrate how the piezoelectric device will move and generate electrical power when deployed on the ocean field. As depicted in Figure 2, the vibration generator is mounted in the vertical position. The constant translation movement from the external source is set in the axial direction. We employed the Analog-to-Digital (A/D) converters to record experimental data by measuring the voltage and displacement. In order to ascertain the distance between the height of the device whenever the vibration is moving up and down, two laser displacement sensors were used. One laser sensor was positioned atop the right end of the device to measure the vibration amplitude at the free side of the piezoelectric device. In contrast, another laser sensor was positioned on the plate above the vibration generator.

Additionally, an accelerometer was affixed to the top of the vibration generator plate to help quantify vibration amplitudes. All of the equipment, as mentioned earlier, was mounted on an aluminum frame structure serving as housing construction. For collecting and saving the whole data for further analysis, a PC is connected to both the A/D converter and the laser sensor.

C. Experiment setup

Figure. 3 demonstrates how piezoelectric device is placed under our experiments setup. The movement of the piezoelectric device came to be in this experiment. In general, two vibration amplitudes will be measured. Since the base model of this device is the cantilever-type piezoelectric, the device is locked on one side, and the other side will be free to move up and down. Both sides measured the amplitude and examined how it would influence electrical power generation.

Figure. 4 shows the illustration from the setup our experiments in this study, while Figure. 5 illustrates in more detail regarding the setup of the piezoelectric device placement, and Figure. 6 displays the actual photo of the setup. As shown in all figures, the piezoelectric device was placed on the top of a vibration generator plate, and its left side was locked with a rubber sponge to make it into a cantilevered piezoelectric device. Meanwhile, the right side of the piezoelectric is not locked, but there is a bottom plate under the device. The distance between the right side of the piezoelectric device and the bottom plate is named the *initial distance* (δ). The (δ) was systematically controlled and experimented upon within a range spanning from 1 cm to 8 cm, with increments of 1 cm. The purpose of this controlled initial distance is to illustrate the ocean conditions where the piezoelectric device is installed as the floating energy harvester device. Therefore, the bottom plate is used as the surface of the ocean water and will limit the full extent of piezoelectric movement.

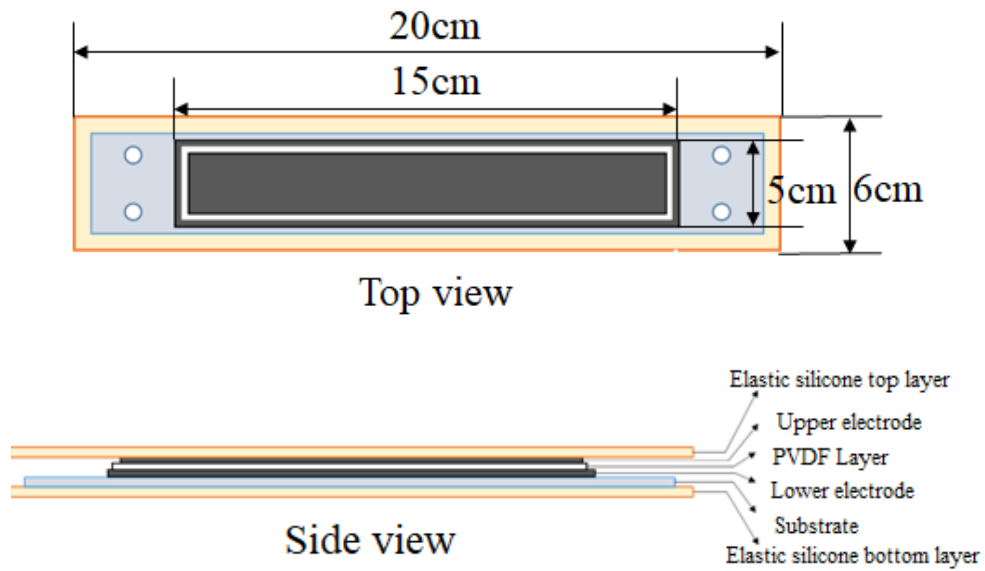


Figure 3. Proposed piezoelectric device. The black area is the PVDF layer while the gray-colored area is the elastic silicone layer.

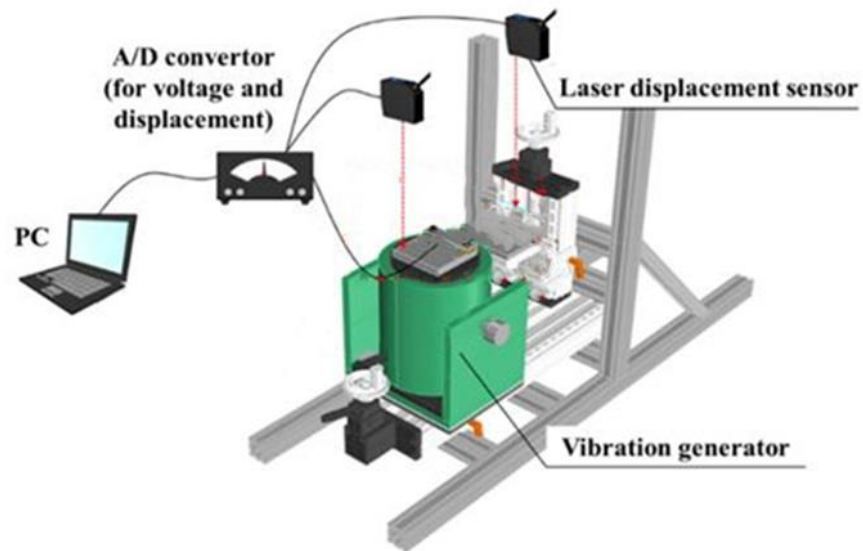


Figure 1. Movement and measuring tools

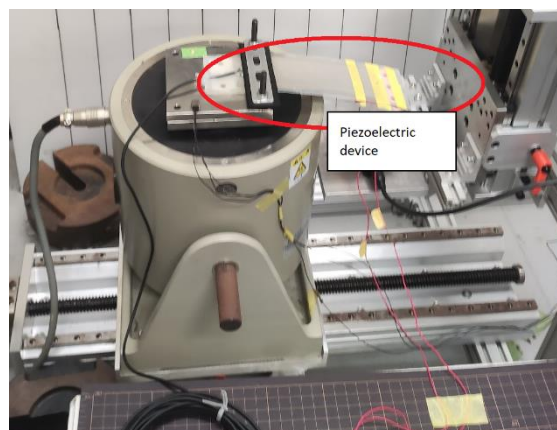


Figure 2. Piezoelectric device placement

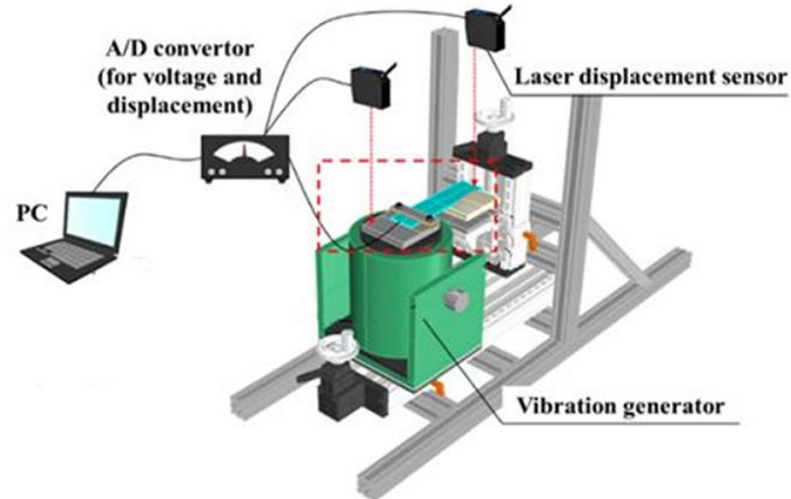


Figure 5. The setup of the piezoelectric device on the movement and measuring tools.

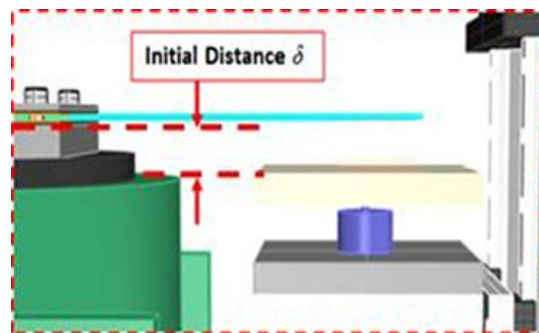


Figure 4. Details of the red box in Figure. 4. The setup of the piezoelectric device.



Figure 6. Top view of the actual experiments setup.

Additionally, the frequency of the vibration generator was set up and tested on 4.0, 6.0, 8.3, 10.0, and 12.0 Hz. The summary of the experiment setup is demonstrated in Table 1.

Also, as mentioned in the previous sub-chapter, the A/D converters and sensors are connected to the PC for data collection and further analysis. Data from each experiment was acquired at one-millisecond intervals over a continuous duration of thirty seconds, yielding a total of

30,001 data points. The value of the electrical voltage from the piezoelectric device is measured and collected from the sensor and converters before being converted into data in the PC. The internal resistance of the A/D converter in an open circuit configuration was configured at one megaohm (1 MW). The computation of electrical power was subsequently carried out utilizing Ohm's law concerning this specific resistance value.

TABLE 1.
 EXPERIMENTAL SETUP FOR THIS EXPERIMENT STUDY

Parameters	Values
Vibration frequency (f)	4.0, 6.0, 8.3, 10.0, 12.0 Hz
Initial distance (δ)	2,3,4,5,6,7,8 cm

III. RESULTS AND DISCUSSION

A comprehensive analysis of piezoelectric generator performance was conducted, and the results of carefully selected experiments are meticulously presented in Figure. 7 to Figure. 10. These figures provide an insightful visualization of the time history and output voltage across various time scales, offering a nuanced understanding of the piezoelectric system's behavior under different conditions.

Figure. 7, in particular, unveils a detailed representation of the outcomes from the Analog-to-Digital (A/D) converter tools, where data is systematically saved on a computer for further scrutiny. In this specific case, with a frequency (f) of 6.0 Hz and the initial distance (σ) of 5.0 cm, Figure. 7 also illustrates the dynamic interplay of the piezoelectric generator, showcasing the entire output voltage spectrum. The graphical depiction serves as a comprehensive overview, allowing researchers and analysts to glean valuable insights into the system's performance.

Upon closer examination of Figure. 7, critical parameters such as the peak and trough voltage become apparent, providing a foundation for in-depth analysis. Discerning these specific values facilitates a more profound understanding of the generator's capabilities and limitations.

The inclusion of various time scales in the graphical representation enhances the interpretability of the results, enabling researchers to discern patterns and trends across different temporal dimensions. This meticulous approach to data visualization contributes to the overall robustness of the study, offering a comprehensive exploration of the piezoelectric generator's behavior under diverse experimental conditions.

In order to find the output voltage average value from the piezoelectric generator, Figure 8. is used as an example. Since there is a chance that the electricity generated from the generator is not yet settled, we observed the value of the output voltage from the last 30 seconds of the experiments (25 s – 30 s). From there, the ten highest values of the output Peak voltage and the ten highest values of the output Trough voltage are then selected. After the selection, the values are changed into an absolute value (no negative). The absolute and average of those 20 highest output values are then used as the “Average Output Voltage” of that particular setup. For example, in the experiment case of ($f = 6.0 \text{ Hz}$, $\sigma = 5.0 \text{ cm}$), Based on the average of the 20 highest values, the Average Output Voltage of the piezoelectric generator is 2.47 volts.

Apart from observing and finding the average output voltage, we also need to verify whether the results of the experiments are in accordance with our setup arrangement. To verify the results, Figure. 9 and Figure.

10 are displayed to help the reader view the verification more easily. Figure. 9 presents the Time history and output voltage from the experiments of ($f = 6.0 \text{ Hz}$, $\sigma = 5.0 \text{ cm}$) for 1 second, while the more detailed graph in Figure. 10 shows the Time history and output voltage from the experiments of ($f = 6.0 \text{ Hz}$, $\sigma = 5.0 \text{ cm}$) for 0.3-second periods. Based on Figure. 9, we can see that the total wave under one second period is six waves. In addition, if we look at Figure. 10, it can be seen that both output voltage peaks at times of 29.786 seconds and 29.952 seconds, which is around 0.16667 seconds time difference. The results of both the “total number of waves per second” and the time difference are in accordance with the experiment setup that utilizes the vibration frequency of 6.0 Hz. Following the results of the 1 case of the experiments, the remaining case are finished with the value of the Average Output Voltage is then sorted on Figure. 11 and Figure. 12.

The discussion regarding the main points of this study is elucidated in the following few paragraphs. Since this study aims to check and verify various factors that could influence the electrical output of the piezoelectric generator, selected parameters are looked upon and compared with the output voltage from the piezoelectric device. To elucidate the authors point of view, Figure. 11 is presented to illustrate the effect of the initial distance while Figure. 12 is presented to illustrate the effect of the vibration frequency to piezoelectric device electrical output.

The initial distance plays a role in determining how wide the piezoelectric could vibrate. As shown in Figure. 5, the initial distance provides a space and obstructions based on the setup. All of our parameters are shown in Table. 1, we found that the piezoelectric device can move without obstruction if the initial distance is more than 3 cm. Based on the information from Figure. 11, it can be seen that the initial distance does not have a linear relationship with the electrical output of the piezoelectric generator. Although it is true that the highest value of the Average Output Voltage (4.5 V) occurs under the highest setup of the initial distance (8 cm), several of the electrical outputs under different frequencies have different highest values on different initial distances. For example, as mentioned before, under the frequency of 6 Hz, the highest output value (4.5 V) is indeed on the highest initial distance (8 cm). However, on a frequency of 12 Hz, the highest output (around 2.5 V) appears at the lowest initial distance (2 cm). Whereas on a frequency of 8.3 Hz, the highest output value (3.0 V) occurred at an initial distance of 4 cm. This proves that the vast space and free area for piezoelectric movement are not always necessary to be wide or as high as possible. The findings suggest that the initial distance is not the primary determinant of the piezoelectric device's electrical performance.

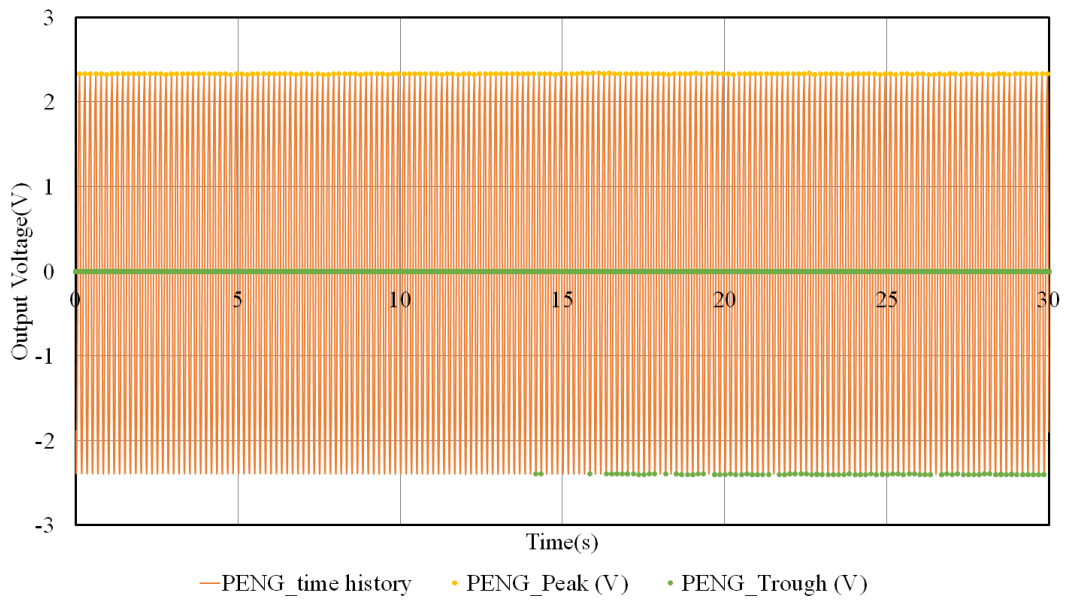


Figure 7. Time History and Output Voltage of the experiments ($f = 6.0 \text{ Hz}$, $\sigma = 5.0 \text{ cm}$) for the whole 30 seconds.

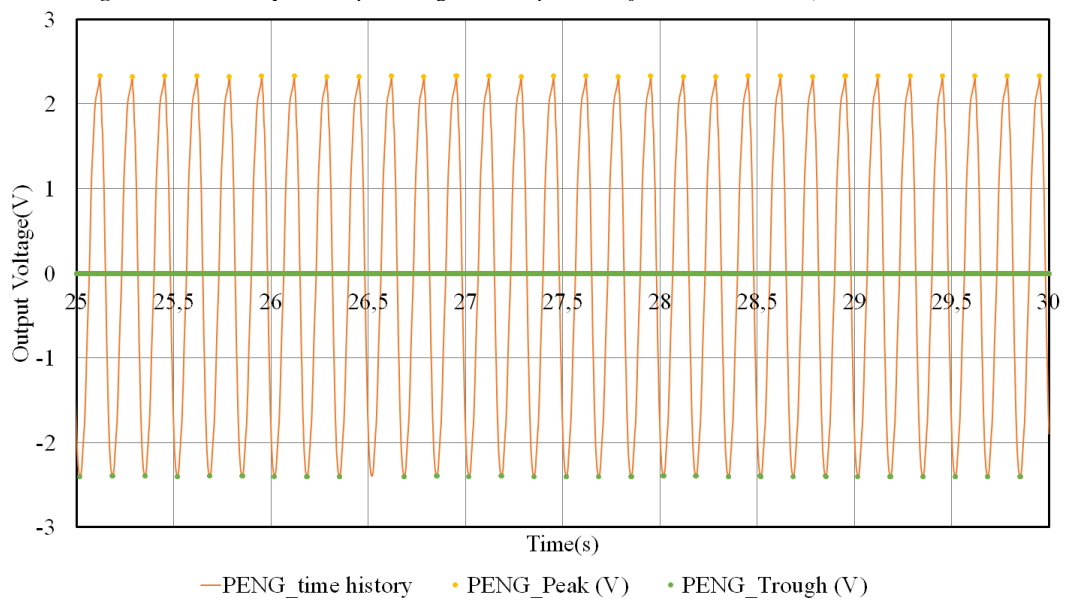


Figure 8. Time History and Output Voltage of the experiments ($f = 6.0 \text{ Hz}$, $\sigma = 5.0 \text{ cm}$) for 5 seconds.

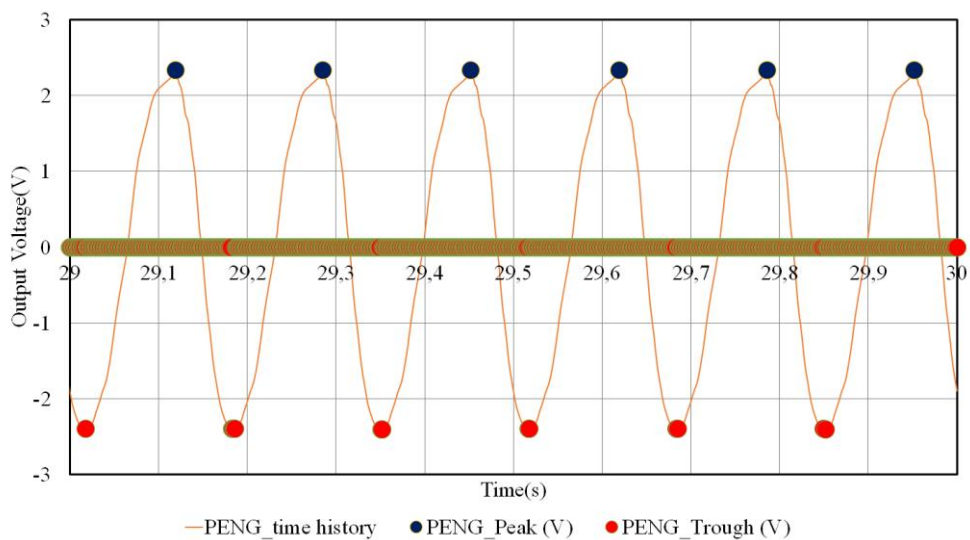


Figure 9. Time History and Output Voltage of the experiments ($f = 6.0 \text{ Hz}$, $\sigma = 5.0 \text{ cm}$) for 1 seconds.

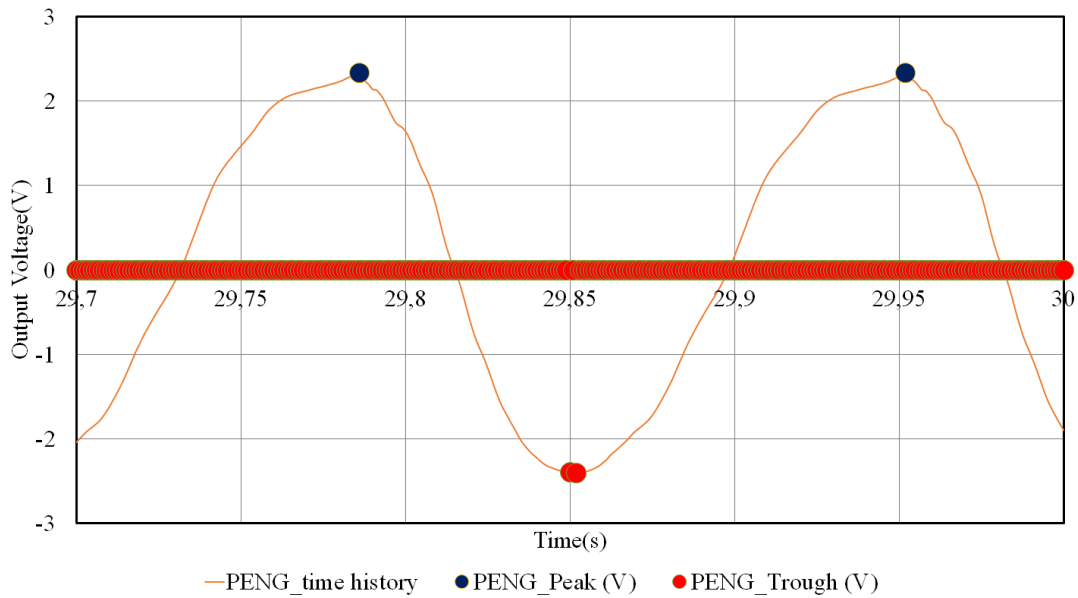


Figure 10. Time History and Output Voltage of the experiments ($f = 6.0 \text{ Hz}$, $\sigma = 5.0 \text{ cm}$) detailed for 6.0 Hz case.

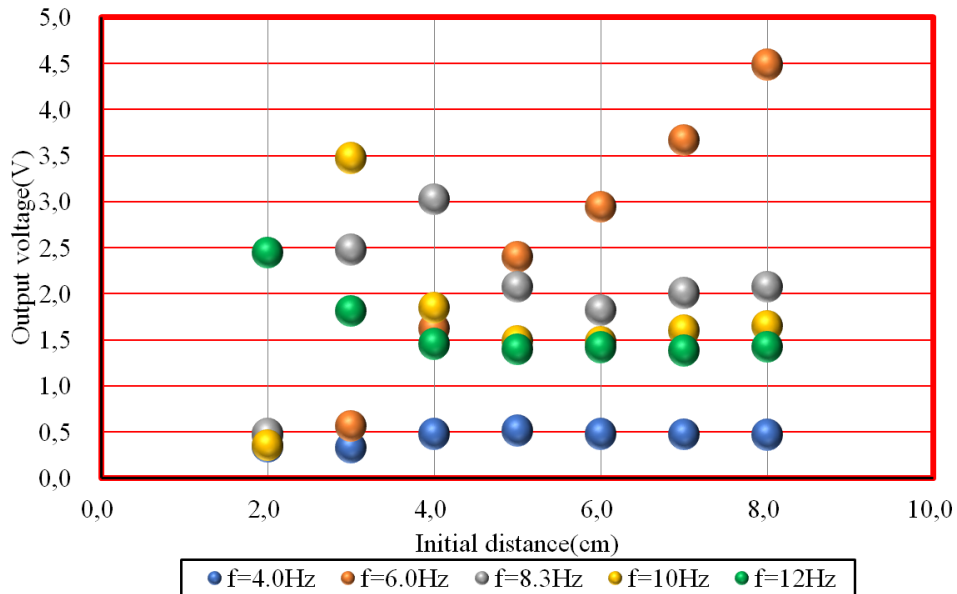


Figure 11. Average Output Voltage of the Piezoelectric under various Initial distance.

This insight provides a valuable foundation for practical applications, indicating that piezoelectric devices can be installed in tight or narrow spaces without compromising their electrical efficiency. Consequently, this research contributes valuable knowledge for the strategic deployment of piezoelectric technology in real-world conditions.

Vibration frequency is also another parameter that we investigated. Figure. 12 presents the piezoelectric average output voltage under various frequencies. Contrary to previous beliefs, vibration frequencies also do not have a linear relationship with the electrical performance of the piezoelectric device. The highest voltage mainly occurs under the frequency of 6.0 Hz. The highest voltage under the frequency of 6.0 Hz occurs for the initial distance of 5-8 cm. Meanwhile, the frequencies representing the highest voltage for the case of initial distance $\leq 4 \text{ cm}$ are different.

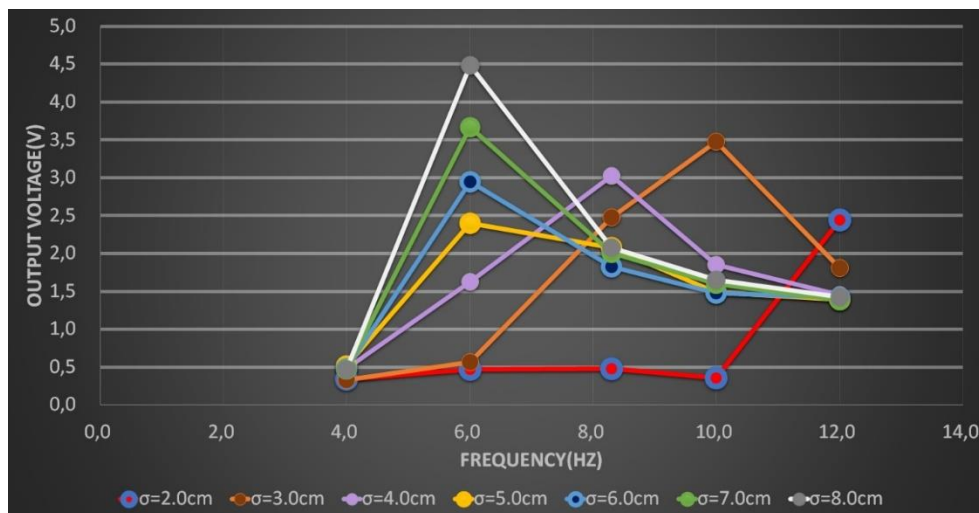


Figure 12. Average Output Voltage of the Piezoelectric under various frequencies.

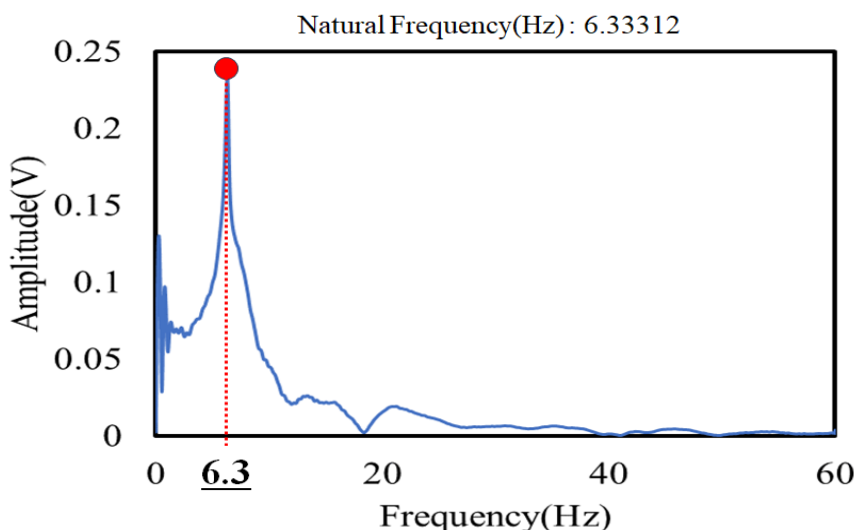


Figure 13. Natural Frequency of our Piezoelectric device model.

For the case of $\sigma=4.0$ cm, the highest voltage occurs at 8 Hz, the case of $\sigma=3.0$ cm is at 10 Hz, while $\sigma=2.0$ occurs at 12 Hz.

Based on the vibration frequency results, we tried to investigate more based on the theory of vibration. We focused on the importance of the observed piezoelectric device's natural and resonant frequency theory. Natural frequencies are the frequency where the object vibrates naturally whenever it is subjected to an external force. On the other hand, the resonant frequency is the specific frequency at which the device vibrates most strongly whenever it is subjected to an external force. Once the vibration frequency from the movement of the piezoelectric device matches its own natural frequency, a resonance will occur, resulting in higher electrical output.

Using the harmonic tool, we found that the piezoelectric device's natural frequency occurs at 6.333 Hz. Therefore, this finding clarifies why most of our experiments' highest electrical output occurs at the vibration frequency of 6.0 Hz. The reason for this is that at the frequency of 6.0 Hz, the piezoelectric is closer to its

natural frequency, resulting in the development of the resonance of the device. With the resonance occurring during the device's movement, the piezoelectric vibrates at its highest, causing a higher electrical output. However, the initial distance also plays an indirect role in the resonance.

If the device has a much thinner or less space to vibrate, the resonance is unlikely to occur since the device will hit the boundary or limitation from the space. Consequently, the tuning and precise selection of the piezoelectric device's distance and frequency must be accurately measured beforehand. In conclusion, the vibration frequency and initial distance generate much higher output from the piezoelectric device. However, the relationship between each parameter and electrical results is not linear; the higher the setup parameters, the higher the results. Both vibration frequency and initial distance need to be tuned following the piezoelectric device's own natural frequency for the resonance to occur and to improve the electrical performance of the proposed piezoelectric generator device.

IV. CONCLUSION

In this study, we elucidate the importance of the natural frequency parameter as one of the central points for improving the electric performance of the piezoelectric generator device. Several vibration frequencies and numerous initial distances (commonly used as main parameters when setting up the device's installation) are also set to illustrate our argument. We found that neither vibration frequency nor initial distance has a linear relationship between those parameters and the result of the piezoelectric's electrical output. The highest result found in the experiment results occurred on the vibration frequency of 6.0 Hz. After several analyses, we found that the vibration frequency is the closest value to the natural frequency of the proposed piezoelectric device used in this study. The resonance observed when these frequencies align demonstrates the necessity for careful consideration and adjustment during the setup process. This finding underscores the significance of thorough investigation and meticulous preparation of the device's installation. In essence, achieving optimal electrical output from the piezoelectric generator necessitates a deliberate alignment of external forces with the natural frequency of the device, emphasizing the need for precision and attention to detail in research and practical applications.

REFERENCE

- [1] X. D. Xie, Q. Wang, and N. Wu, "Energy harvesting from transverse ocean waves by a piezoelectric plate," *Int. J. Eng. Sci.*, vol. 81, pp. 41–48, 2014, doi: 10.1016/j.ijengsci.2014.04.003.
- [2] N. Wu, Q. Wang, and X. D. Xie, "Ocean wave energy harvesting with a piezoelectric coupled buoy structure," *Appl. Ocean Res.*, vol. 50, pp. 110–118, Mar. 2015, doi: 10.1016/j.apor.2015.01.004.
- [3] K. H. Kim, S. B. Cho, H. D. Kim, and K. T. Shim, "Wave power generation by piezoelectric sensor attached to a coastal structure," *J. Sensors*, vol. 2018, 2018, doi: 10.1155/2018/7986438.
- [4] C. Tuma and D. Phaoharuhansa, "Ocean wave energy harvest using multi-piezoelectric cantilever beams," *Int. J. Mech. Eng. Robot. Res.*, vol. 9, no. 6, pp. 911–916, 2020, doi: 10.18178/ijmerr.9.6.911-916.
- [5] J. Kan, C. Fan, S. Wang, Z. Zhang, J. Wen, and L. Huang, "Study on a piezo-windmill for energy harvesting," *Renew. Energy*, vol. 97, pp. 210–217, 2016, doi: <https://doi.org/10.1016/j.renene.2016.05.055>.
- [6] X. D. Xie, Q. Wang, and N. Wu, "Potential of a piezoelectric energy harvester from sea waves," *J. Sound Vib.*, vol. 333, no. 5, pp. 1421–1429, Feb. 2014, doi: 10.1016/j.jsv.2013.11.008.
- [7] G. W. Taylor, J. R. Burns, S. A. Kammann, W. B. Powers, and T. R. Welsh, "The Energy Harvesting Eel: a small subsurface ocean/river power generator," *IEEE J. Ocean. Eng.*, vol. 26, no. 4, pp. 539–547, 2001, doi: 10.1109/48.972090.
- [8] U. Latif *et al.*, "Experimental investigation of energy harvesting eel in the wake of bluff body under ocean waves," *Proc. Inst. Mech. Eng. Part M J. Eng. Marit. Environ.*, vol. 235, no. 1, pp. 81–92, Aug. 2020, doi: 10.1177/1475090220949334.
- [9] F.-R. Liu, W.-M. Zhang, Z.-K. Peng, and G. Meng, "Fork-shaped bluff body for enhancing the performance of galloping-based wind energy harvester," *Energy*, vol. 183, pp. 92–105, 2019, doi: <https://doi.org/10.1016/j.energy.2019.06.044>.
- [10] H. Liang, G. Hao, and O. Z. Olszewski, "A review on vibration-based piezoelectric energy harvesting from the aspect of compliant mechanisms," *Sensors Actuators, A Phys.*, vol. 331, p. 112743, 2021, doi: 10.1016/j.sna.2021.112743.
- [11] H. Liu, J. Zhong, C. Lee, S. W. Lee, and L. Lin, "A comprehensive review on piezoelectric energy harvesting technology: Materials, mechanisms, and applications," *Appl. Phys. Rev.*, vol. 5, no. 4, 2018, doi: 10.1063/1.5074184.
- [12] J. Briscoe and S. Dunn, "Piezoelectric nanogenerators - a review of nanostructured piezoelectric energy harvesters," *Nano Energy*, vol. 14, pp. 15–29, Oct. 2014, doi: 10.1016/j.nanoen.2014.11.059.
- [13] P. Jiao, "Emerging artificial intelligence in piezoelectric and triboelectric nanogenerators," *Nano Energy*, vol. 88, p. 106227, 2021, doi: 10.1016/j.nanoen.2021.106227.
- [14] N. V. Viet, N. Wu, and Q. Wang, "A review on energy harvesting from ocean waves by piezoelectric technology," *J. Model. Mech. Mater.*, vol. 1, no. 2, 2017, doi: 10.1515/jmmm-2016-0161.
- [15] E. M. Wardhana *et al.*, "Harvesting ocean energy using a hybrid type of nanogenerator with PENG and TENG," *The 31st International Ocean and Polar Engineering Conference*, p. ISOPE-I-21-1247, Jun. 20, 2021.